Electrical Power and Energy Systems 176 (2026) 111705

Contents lists available at ScienceDirect

International Journal of Electrical Power and Energy Systems

journal homepage: www.elsevier.com/locate/ijepes

Quantifying stator winding fault severity in induction motors: A machine learning approach with spectral feature extraction

Rehaan Hussain [a,c,*], Mohammed Yaqoob [a,c], Mohammed Ishaq [a,c], Mohammad Alshaikh Saleh [a,d], Shady S. Refaat [b,e]

[a] Student Member, IEEE
[b] Senior Member, IEEE
[c] Electrical and Computer Engineering, Texas A&M University at Qatar, Doha, Qatar
[d] Electrical and Computer Engineering, Texas A&M University, College Station, TX, 77843, USA
[e] School of Physics, Engineering & Computer Science, University of Hertfordshire, Hatfield, United Kingdom

ARTICLE INFO

Keywords:
Fault detection
Predictive maintenance
Wavelet transform
Feature extraction
Electrical fault diagnosis

ABSTRACT

Induction motors (IMs) constitute a fundamental component of industrial infrastructure, accounting for approximately 60%–70% of global industrial energy consumption and driving critical manufacturing processes. The proliferation of electrical faults in electric motors, particularly in their incipient stages, presents significant challenges to operational reliability and energy efficiency, necessitating advanced fault diagnostic methodologies. The challenge lies in detecting the incipient fault in its early stages, as there is minimal damage and it may not be easily detectable. This paper introduces a novel machine learning-based framework for quantifying stator winding fault (SWF) severity in IMs through multi-domain signal analysis. The proposed methodology implements a hybrid feature extraction approach, integrating Fourier and wavelet transform coefficients derived from three-phase current signals to capture both frequency-domain characteristics and localized time–frequency patterns indicative of electrical degradation, along with statistical features. The experimental validation incorporates a diverse range of machine learning architectures, spanning traditional algorithmic approaches such as Support Vector Machines (SVMs) and advanced ensemble methodologies including Histogram Gradient Boosting (HGBM) and XGBoost (XGB). The proposed framework demonstrates superior fault detection capabilities, achieving classification accuracy exceeding 95% across multiple evaluation metrics including precision (0.9952), recall (0.9949), and F1-score (0.9952), which is an extremely high score for a multiclassification model of four classes in signals. Furthermore, SHapley Additive exPlanation (SHAP) is used to recognize the important features that led to the success of the models. The obtained results establish the efficacy of machine learning techniques in facilitating early fault detection and enabling condition-based maintenance strategies, thereby enhancing operational reliability in industrial applications. To promote reproducibility and facilitate further research in this domain, the complete implementation framework, including source code, is made publicly available in https://github.com/rehaan-hussain/Quantifying-Electrical-Severity-in-Induction-Motors-A-Machine-Learning-Approach.

1. Introduction

IMs are indispensable in modern industrial applications, providing essential mechanical power across various sectors, including manufacturing, transportation, and energy. As the backbone of industries, they play a pivotal role in driving machinery and operations, accounting for over 60% of industrial energy consumption globally in 2022 [1]. Given their significance, maintaining IM efficiency and performance is vital for operational continuity and cost-effectiveness. Despite their resilience, IMs are susceptible to various faults that can severely impact their performance. In general, the faults are categorized based on their time characteristics into three types: abrupt, incipient, and intermittent. These faults are generally categorized into electrical and mechanical faults [2]. Electrical faults, especially incipient ones, pose a significant challenge as they often degrade motor components over time, leading to eventual motor failure if not detected early. Proactive fault detection is essential to avoid costly downtimes and extend motor

* Corresponding author.
E-mail address: rehaan.hussain@qatar.tamu.edu (R. Hussain).

https://doi.org/10.1016/j.ijepes.2026.111705
Received 10 July 2025; Received in revised form 20 December 2025; Accepted 13 February 2026
Available online 12 March 2026
0142-0615/

lifespan towards a more sustainable outcome for energy consumption and financial concerns.

SWFs are the second most prevalent type of malfunction in IMs, surpassed only by bearing faults [3]. Representing 38% of all faults in IMs, their high occurrence underscores the critical need for effective detection mechanisms to mitigate such failures [4]. SWFs can arise from various issues, including lamination defects such as core overheating or slackening, and frame-related problems such as earth faults and circulating currents. Additionally, more common issues involve local damage and contamination of insulation, turn-to-turn faults, and short circuits between line-to-line currents caused by partial discharge [5]. These damages are caused due to several reasons. Thermal stresses are due to voltage variations, unbalanced phase voltage, cycling overloading and high temperatures. Additionally, a more direct cause could be electrical stresses which can be tracking, corona and transient voltage conditions, causing degradation to the insulation material of the windings, thus affecting the magnetic field rotation in the stator.

The rapid advancements in artificial intelligence (AI), particularly in machine learning (ML), have positioned these technologies as powerful tools for addressing industrial challenges, including fault detection in IMs. AI-driven solutions ensure real-time monitoring and predictive maintenance, which are critical for preventing unforeseen breakdowns, ensuring operational efficiency and enhancing the longevity of the assets. With its ability to analyze complex patterns in motor signals, ML offers unprecedented accuracy in detecting early-stage faults.

SHAP is a game theory approach to enhance the underlying concept of an ML model. Connecting the importance of features that leads to high values in metrics provides the foundation for reliability in these models. Using SHAP explanations increases the credibility of an ML model in a practical application, as researchers may not be able to easily interpret algorithms that are open-source. Thus, building a solid understanding of features using explainable AI increases the integrity of the model use.

In this work, the problem of detecting SWF severity in IMs through ML by leveraging spectral features extracted from current signals has been addressed. By applying both Fourier and wavelet transform coefficients, the critical frequency-domain and time–frequency characteristics are captured which are indicative of motor degradation in the variational signal changes and observe incipient fault growth in the current. These features, when combined with statistical descriptors, provide a comprehensive representation of motor health.

This study shows a comparative analysis of ML models that detect several varying electrical severities in IMs using a combination of signal processing methods, namely Fourier coefficients (FC) and wavelet Coefficients (WC). By exploring the combination in this domain, a sliding-window feature extraction strategy is proposed to capture localized characteristics, enabling effective identification of both transient and steady-state behaviors, leading to a high performance output. Through extensive experimentation across multiple ML models, almost all the models achieved over 95% accuracy in fault detection and severity classification. Furthermore, the integration of explainable AI, specifically SHAP, provides valuable insights into the usefulness of each feature by its contributions, allowing interpretability and transparency of proposed approach.

The remainder of the paper is structured as follows. Section 2 reviews related work in the field of fault detection with ML techniques for IMs. In Section 3, the methodology, including data preprocessing, feature extraction, and the novel ML approach with spectral feature extraction approach is proposed. Section 4 presents the results, followed by an analysis and discussion in Section 5. Finally, Section 6 concludes the paper with a summary of findings and suggestions for future work.

2. Machine learning applications

Stator winding faults in IMs have been extensively studied in the literature, highlighting various ML approaches to detect SWF for IMs. For instance, in [6], the authors proposed a soft voting ensemble ML algorithm comprising eight models, designed to extract the max–min difference value of current signals. This approach was rigorously evaluated using 10-fold cross-validation, achieving an average accuracy of 96%. In [7], various ML models were experimented with using polar magnetic symmetry induced in finite element method (FEM) software which earned 88% accuracy and above. In [8], a fault detection system for short circuit faults using current envelope energy with Akima interpolation is proposed, achieving 96.9% with SVM for healthy or faulty binary classes. In [9], a study on three-phase squirrel cage IMs for inter-turn faults in the incipient stage was conducted, utilizing a genetic algorithm to estimate values of parameters such as stator and rotor resistances and mutual inductance, identifying the localized fault due to variations in the signal obtained. In [10], the authors proposed the usage of wavelet packet transform implemented in MATLAB by using sub-bands of the signal used to identify the severity of the SWF. In [11], an artificial neural network (ANN) fault detection algorithm is proposed considering the utilization of discrete wavelet energy ratio with an artificial neural network such as multi-layer perceptron, radial basis function, and Elman neural network (ENN) for inter-turn short circuit fault detection in three-phase IMs. Using mean squared error as the evaluation metric, the ENN has emerged on top in terms of high accuracy. The authors in [12] detect stator winding faults by utilizing discrete wavelet transform (DWT) to analyze current signals in the time domain. While their approach demonstrated novelty in its signal processing methodology, it did not incorporate ML algorithms for SWF detection. In contrast, [13] employed Park's transformation to convert three-phase stator currents into RGB images, which were then processed using a convolutional neural network designed by the authors, termed RPCNNet. This deep learning-based method achieved a remarkable accuracy of 98.24%. The authors of [14] proposed a fuzzy neural network system on the analysis of the electromagnetic field of the solid rotor in IMs to develop an approach to detect and diagnose stator winding faults. The proposed technique was able to fully classify healthy and inter-turn fault states and achieved 98% with phase to ground fault state. [15] published a work using MCSA on SWF using FFT, spectrogram and scalogram to detect said faults with the help of deep learning methods, specifically long short-term memory (LSTM) models. Known for working extremely well with continuous data, LSTM was able to achieve 97.87% accuracy in fault classification. [16] used Stockwell transform to detect various motor conditions like inter-turn shorts and phase to ground faults by decomposing current signals into matrices which were fed into Support Vector Machine (SVM) for fault detection achieving approximately 96% accuracy for both types of faults.

In addition to conventional time-domain or single-domain spectral features, several works have demonstrated that combining Fourier and wavelet representations provides richer fault-related information. Fourier coefficients capture the global harmonic distortions associated with imbalance and circulating fault currents, whereas wavelet coefficients are sensitive to localized, non-stationary transients that accompany early insulation breakdown. Prior studies on IMs have shown that these two feature types are complementary. [17] extracted both Fourier and wavelet features from stator current signals and reported improved separability across multiple motor fault classes when the fused feature set was used, compared to either transform alone. Similarly, the authors in [18] employed a wavelet–Fourier hybrid representation for rotating machinery vibration data and demonstrated higher diagnostic effectiveness relative to traditional frequency-only approaches. While these studies underline the benefit of multi-domain spectral features for fault detection, they do not explicitly quantify fault severity levels or evaluate early incipient stages. The present work

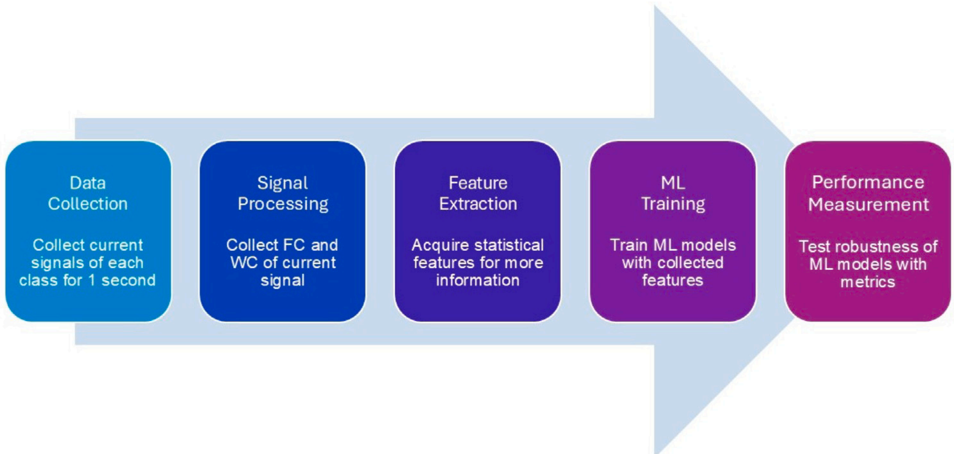

Fig. 1. Methodology of proposed approach.

builds upon this foundation by integrating Fourier and wavelet coefficients specifically for severity classification of stator inter-turn faults, enabling data-driven estimation of progressive degradation rather than simple healthy-versus-faulty discrimination.

The existing literature highlights the importance of classifying and detecting various types of SWFs in induction machines. However, a significant gap remains in assessing the severity of these faults, particularly in quantifying the progression of incipient faults. Incipient faults, characterized by gradual degradation over extended periods rather than immediate failure, can cause substantial damage if not identified promptly. Early and accurate diagnosis of such faults in industrial settings allows IMs to be disconnected from the grid and repaired during scheduled maintenance periods, thereby preventing unplanned breakdowns and minimizing operational downtimes. While ML models have shown promise in enhancing fault detection, their practical implementation in industrial scenarios is often hindered by the high computational demands of deep learning approaches or the use of unconventional ML models. Moreover, the limited availability of open-source codes in the literature further complicates the adoption of these methods, presenting an additional barrier to their widespread application.

3. Methodology

This section presents a comprehensive framework for detecting and quantifying electrical severity in induction motors through machine learning techniques. The proposed methodology encompasses three primary components: data preprocessing for signal quality enhancement, feature extraction for capturing fault signatures, and the implementation of machine learning algorithms. The framework is designed to ensure robust fault detection while maintaining computational efficiency and generalization across various operational conditions. The approach in this paper is represented in Fig. 1, where we acquire data from an experimental setup for different levels of severity in the stator winding fault. The stator current signals are sampled at 12 kHz using a VIBDAQ 4+ data acquisition card. This device features four independent 24-bit A/D converters, ensuring exceptional phase matching across channels. The acquired data is then transmitted to a laptop via a USB connection for further processing. Feature engineering is applied, namely signal processing techniques to enhance class generalization according to the signals, such as the Fourier and WC. Features are then extracted from the current data, such as mean, median, and statistical features of all the three phases. Finally, the ML models are trained and their accuracies, precision, recall, cross-validation across accuracy, receiver operating curves (ROC) and precision recall curves (PRC) are acquired. These metrics are used to measure the validity of the model in application.

3.1. Data preprocessing

The experimental dataset comprises three-phase current measurements: I_A, I_B, I_C, sampled at 10 kHz, along with corresponding fault labels that quantify the severity of electrical anomalies present in the system. The preprocessing pipeline incorporates multiple stages to ensure data integrity and optimal representation for subsequent analysis. The initial stage implements a dual-approach outlier detection strategy: a Z-score method with a threshold of 3σ for identifying global anomalies, complemented by Tukey's Fences methodology that flags values exceeding 1.5 times the interquartile range (IQR). This comprehensive approach identified and eliminated approximately 1.2% of anomalous data points that could potentially compromise model performance.

To facilitate comparative analysis of normalization impacts on model performance, the dataset was maintained in both raw and normalized formats. The normalization process employed min–max scaling on the three-phase current signals (I_A, I_B, I_C), mapping the values to a [0,1] range while preserving the relative relationships between phases. This standardization prevents any phase from exercising disproportionate influence on the learning algorithm due to magnitude differences. The preprocessing pipeline addressed missing values, which constituted 0.5% of the dataset, through median imputation, a method selected for its robustness against skewed distributions and outlier resistance. The preservation of both normalized and non-normalized datasets enabled rigorous evaluation of scaling effects on fault detection accuracy under various operational conditions. The final dataset size left to work was 479,232 samples with 110,592 samples for the healthy class and 73,728 samples for each fault class. This indicates an extreme class imbalance. Since the samples needed to train a model to be robust were adequate, this imbalance was taken into account when continuing with the experiments.

The different fault severity percentages showcase the approximate proportion of damage existing in the stator winding turns short-circuited due to insulation degradation, rather than an exact fixed value. However, in practice, these may differ in ranges of $\pm 0.5\%$ as the number of shorted turns rarely remains whole numbers. For instance, a 1% fault may relate to one shorted turn out of 64. While higher percentages correspond to great insulation resistance drop and higher currents. Therefore, the more the percentage increases, the greater the thermal stress, magnetic imbalance and further damage to the internal components of the induction motor, making early fault detection in windings a critical aspect of lifetime estimation and elongation.

3.2. Feature extraction

The feature extraction framework implements a multi-domain approach to capture comprehensive fault signatures from the preprocessed current signals. The framework integrates statistical, frequency-domain, and time–frequency domain features to ensure robust fault characterization across various operational conditions. However, the experimental fault levels that are collected in percentages are not characterized by international standards such as IEC or NEMA. These standards recommend intervention when measurable metrics indicate critical limits, such as abnormal temperature rise beyond insulation class limits or current imbalances exceeding 5%–10%, which are associated with rising stator temperatures and torque reduction. The data utilized for this paper was artificially induced to simulate a fault in the current signatures for ML purposes. While direct short circuits are not recognized globally for fault detection, this paper aims to imitate insulation faults in varying resistances, affecting the characteristics of the signals collected. The different ranges of the fault as the gradual increase in deterioration takes place allows operators to make informed decisions in scheduling motor downtimes in the industry.

Statistical features computed for each phase include first-order metrics (mean, median, mode) and higher-order moments (variance, skewness, kurtosis). While these features effectively capture overall signal characteristics and distribution patterns, their limitation in representing transient phenomena and frequency-specific fault signatures necessitated the incorporation of spectral analysis techniques.

The spectral analysis framework employs both Fourier and wavelet transforms to capture complementary aspects of the fault signatures. The Discrete Fourier Transform (DFT) implementation extracts the first 20 Fourier coefficients (FC) from each phase (I_A, I_B, I_C), focusing on the fundamental frequency components and harmonics that typically manifest during electrical faults. This frequency-domain representation enables the identification of periodic fault patterns and harmonic distortions characteristic of specific fault types.

The framework implements the Discrete Wavelet Transform (DWT) using the Daubechies 6 (db6) [19,20] wavelet basis to capture localized transient events and non-stationary signal components. The selection of db6 wavelet was motivated by its optimal time–frequency localization properties and demonstrated effectiveness in electrical fault analysis. The wavelet decomposition generates 20 coefficients per phase, providing multi-resolution analysis capability crucial for detecting short-duration fault events and intermittent anomalies.

The feature extraction process implements a sliding window mechanism with a width of 50 samples and 50% overlap between consecutive windows. This approach generates a feature vector comprising 120 elements (20 FC + 20 WC × 3 phases) for each window position. The overlapping window strategy ensures temporal continuity in feature representation while capturing both steady-state and transient fault behaviors. The extracted features include 2 spectral features (Fourier Transform and Wavelet Transform) and 2 time–frequency features (STFT and WPT), offering a comprehensive representation of the signal. For machine learning model development, the dataset is divided into training (80%), and testing (20%) splits, ensuring reliable model performance evaluation and fault severity quantification.

The combination of FC and WC proves to be a superior fault representation because of FC capturing global harmonic distortions in electrical faults in the frequency domain and WC acquiring localized time–frequency information essential for detecting transient and incipient fault components, making their combination more informative than using either technique alone.

3.3. Machine learning algorithms

Following feature extraction, various ML algorithms were applied to classify the faults within the induction motor system. The extracted features, which are statistical, Fourier, and WC, were used as inputs to these models. Various algorithms were explored, including traditional classifiers such as Logistic Regression [21], Multi-Layer Perceptron (MLP) [22], Linear Discriminant Analysis (LDA) [23], Quadratic Discriminant Analysis (QDA) [24], K-nearest Neighbors (KNN) [25], Decision tree [26], Random Forest (RF) [27], XGB [28], CatBoost [29], Gaussian Naive Bayes [30], Stochastic Gradient Descent [31], Extra Trees [32], Passive Aggressive [33], Perceptron [34], Ridge [35], Bagging [36], AdaBoost [37], and HGBM [38]. The choice of models and their hyper-parameters were fine-tuned using Grid search to ensure optimal generalization performance, and cross-validation was performed to validate the metric values like accuracy, precision and F1-score. Model performance was evaluated using accuracy, precision, recall, and F1 score, with the final model selection based on its ability to balance accuracy. The following proposed models were analyzed for their performance by measuring the aforementioned metrics.

1. **Random Forest:** Random Forest (RF) is an ensemble learning algorithm that combines multiple decision trees to improve predictive performance through a process known as bagging. Each tree is trained on a bootstrapped subset of the original dataset, with random subsets of features considered at each split. This randomness introduces diversity among the trees, reducing overfitting and enhancing generalization. During training, decision thresholds are computed for each feature at a given node to split the data recursively until leaf nodes are reached, where predictions are made. The final output of the model is determined by majority voting across all trees. Since this project addresses a classification problem, RF stands a considerable chance at identifying the different severity of SWF because it is well-known for handling non-linear data, which falls under spectral features, and its ability to handle large datasets that may have robust to noisy data.
RF's aggregation of diverse decision trees provides robustness against missing data, as predictions can be made using the available features in each tree. To calculate the split in a decision tree, the entropy is computed using all features based on the following equation to find the threshold [39].
$$H(X) = -\sum_{i=1}^{n} P(x_i)\log_b P(x_i)$$
Additionally, the algorithm is computationally efficient due to its capacity for parallelization, as each tree operates independently of others. This combination of diversity, robustness, and scalability makes RF a powerful tool for classification and regression tasks [40].
2. **Extremely Randomized Trees (Extra Trees):** Extremely Randomized Trees (Extra Trees) is an ensemble learning algorithm that introduces additional randomness into the tree-building process compared to RF. Similar to RF, Extra Trees employs a bagging technique, where multiple decision trees are trained on bootstrapped subsets of the data. However, the key distinction is how the splits of a tree are determined during its construction. The split refers to the threshold at which a condition needs to be met for one leaf versus the other, and this is computed during the training process. While RF calculates the optimal threshold for splitting at each node, Extra Trees selects the splitting point randomly for each feature. This added randomness reduces the computational complexity of the model, significantly decreasing training time.
Despite its increased randomness, ExtraTrees maintains robust predictive performance, benefiting from the diversity introduced by the random splits. This approach is particularly advantageous in scenarios with large datasets where computational efficiency is critical. Increasing randomness by maximizing information by increasing the variance. When you feed the ML model with maximum information, the algorithm becomes more robust in

identifying faults. By balancing simplicity and accuracy, Extra Trees serves as a compelling alternative to RF for tasks requiring scalable and efficient learning algorithms [41]. ExtraTrees can prove useful in the identification of multiclass severity faults using an extra randomization method which adds to the robustness factor of the model.

3. **Multilayer Perceptron:** An MLP is the extension of a perceptron, which is a single neuron. MLP works by combining multiple neurons in the format of layers, each with its own biases and weights connecting all the neurons together, forming a network. Each node is a linear equation influenced by the input and the bias it is set to [42].

$$y = \sum_{i=1}^{n} (w_i \cdot x_i) + b$$

Where y stands for the weighted output, w is the weight, x is the input, and b is the bias. Each node contains values consistent with the above equation. To introduce non-linearity, the output of a layer is passed through an activation function, which decides the value. Based on the complexity of the problem, MLPs can perform classification with an appropriate dataset and well-adjusted hyper-parameters. The loss function is calculated by comparing the predicted output to the actual label, which can be optimized using techniques such as SGD or Adam optimizer. The concept introduces learning using mathematical concepts where each feature provides information to the network and makes a decision. Since MLP uses a learning approach, its strength lies in its finetuning feature, which adjusts the model parameters according to the equation above based on what is fed to it. The loss function is steadily decreased using the formula below [43]:

$$\theta = \theta - \eta \frac{\partial J(\theta)}{\partial \theta}$$

4. **XGBoost:** Gradient boosting machine is an algorithm which combines multiple weak learners sequentially into one strong learner. Each model is trained to minimize the loss function from the previous model using gradient descent.
where θ stands for the weight to optimize, η stands for the learning rate at which the value increases or decreases, and $\frac{\partial J(\theta)}{\partial \theta}$ stands for the gradient of the loss function. Gradient boosting can use a wide range of base learners, which can be chosen according to the real world problem meant to be solved. It is considered to be robust due to its flexibility with weights, making it less sensitive to outliers. XGB, standing for Extreme Gradient Boosting, is an optimized algorithm designed for efficiency and adapts to large datasets. Similarly to RF, it is able to handle missing values, supports parallelization and uses decision trees. XGB implements regularization to simplify its model and comes with a built-in cross validation method, thus allowing for observation of overfitting should it occur. The concept of combining weak learners to produce a strong learning model increasing its robustness as its theoretical approach should enable high accuracy classification for SWF.
5. **Histogram Gradient Boosting:** HGBM is a gradient boosting model that supports the use of large datasets as well. It is a variant that capitalizes on discretizing continuous input features into bins that can be considered as histograms, leading to reduction in computational complexity and memory allocation. It follows the same theory of gradient boosting models. Since its structure is similar to XGB, the same advantages apply for SWF severity classification.
6. **Categorical Boosting (CatBoost):** Also a gradient boosting model, CatBoost works by iteratively building trees, efficiently handling categorical features and preventing overfitting. It works well with large datasets, as has been observed with most gradient boosting models.

4. Results

4.1. Signal processing results

The current signals obtained experimentally from the IM were analyzed to extract a comprehensive set of features. These included FC (1–20) and WC (1–20) for each of the three phases. In addition, statistical and signal processing features were computed, including row-wise mean, standard deviation, variance, skewness, kurtosis, signal energy, and features derived from the first and second differentials of the signals. This enriched dataset, comprising the extracted features and the raw IM current signals, was subsequently used to train the ML models.

Fig. 2 provides a comparative visualization of the signals, highlighting the extracted features. Figs. 2(a), 2(c), and 2(e) highlight the normal signals, while Figs. 2(b), 2(d), and 2(f) correspond to their respective fault classes, including the processed signals. The accompanying Fourier and wavelet coefficient plots for each signal reveal distinct patterns. Notably, the Fourier coefficient decomposition produces exclusively non-negative values, in contrast to the wavelet decomposition, which includes both positive and negative values. These differences underscore the complementary nature of Fourier and wavelet analyses in capturing signal characteristics.

In the normal signals, the waveforms show smooth, continuous behavior, with Fourier coefficients showing distinct, consistent peaks and troughs. The wavelet decomposition, performed using the db6 wavelet with a decomposition level of 3, captures both high and low-frequency components in the signal. Notably, the db6 wavelet is effective in detecting subtle changes in the signal by offering a fine balance between time and frequency resolution.

In contrast, the fault signals exhibit deviations from the normal behavior, often characterized by irregular fluctuations or spikes. The Fourier coefficient decomposition for the faulty signals produces non-negative values, showing altered frequency components indicative of the fault's impact on the signal. The wavelet decomposition for the faulty signals includes both positive and negative coefficients, providing a more detailed view of the signal's disruption. The differences in Fourier and wavelet decompositions between the healthy and faulty signals highlight how each method captures distinct signal features, with Fourier coefficients revealing global frequency characteristics and wavelet coefficients offering detailed local variations.

The use of the db6 wavelet and 3-level decomposition ensures that both coarse and fine details of the signal are captured, which is crucial for fault detection in real-time applications. These complementary analyses, combining the global frequency information from Fourier transforms and the localized time–frequency insights from wavelets, provide a robust framework for distinguishing between normal and faulty conditions in the signal.

4.2. Model comparison

The evaluation framework implemented a comprehensive assessment of multiple machine learning architectures leveraging the multi-domain feature space comprising FC, wavelet transformations, and statistical descriptors. The experimental validation encompassed 450,000 feature vectors, necessitating careful consideration of both model performance metrics and computational efficiency for practical deployment scenarios. Table 1 presents a systematic comparison of model performance across multiple evaluation criteria.

The ensemble-based architectures, specifically Extra Trees, Random Forest, and gradient boosting variants (XGB, CatBoost, HGBM), alongside the neural network implementation (MLP), demonstrated superior classification capabilities with accuracy metrics exceeding 98%. This performance level indicates robust fault severity classification across varying operational conditions, with minimal misclassification

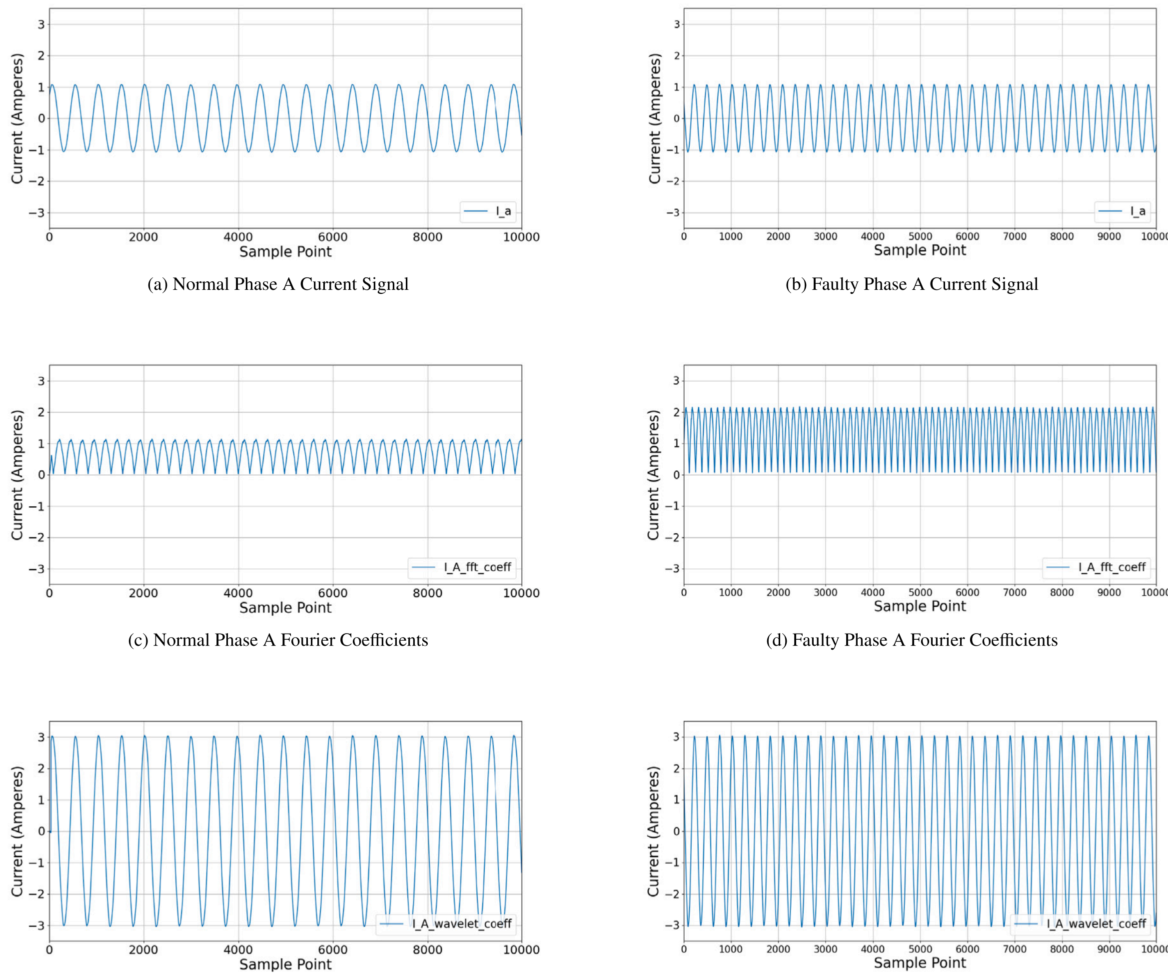

(a) Normal Phase A Current Signal

(b) Faulty Phase A Current Signal

(c) Normal Phase A Fourier Coefficients

(d) Faulty Phase A Fourier Coefficients

(e) Normal Phase A Wavelet Coefficients

(f) Faulty Phase A Wavelet Coefficients

Fig. 2. Comparison between normal and 1% fault.

instances. The model evaluation framework implemented k-fold cross-validation with k=5 to ensure statistical validity and assess generalization capability, effectively mitigating potential overfitting concerns during the training phase.

The performance assessment methodology incorporated multiple complementary metrics to ensure a comprehensive evaluation alongside accuracy such as precision and F1 score. The precision metric quantifies classification accuracy by computing the ratio of true positive predictions to total positive predictions, providing insight into the model's ability to avoid false positive classifications. The recall metric evaluates the model's sensitivity in identifying fault conditions by calculating the ratio of correctly identified positive instances to total actual positive instances. The F1-score, computed as the harmonic mean of precision and recall, provides a balanced assessment of model performance, particularly valuable in scenarios with varying fault severity distributions. This multi-metric evaluation framework enables systematic comparison of model capabilities while considering the practical implications of deployment in industrial environments.

4.3. Precision–recall and receiver operating curves

To further validate the performance of the trained models, PRC and ROC curves were analyzed. The PRC visualizes the trade-off between precision and recall across various threshold values, providing insights into the balance between correctly identified positives and false positives. A higher area under the PRC (AUPRC) indicates a model's ability to distinguish positive cases while minimizing false positives effectively. Higher PRC values near the top-right corner suggest robust model performance, which is observed across the top six models: Extra Trees, RF, MLP, HGBM, CatBoost, and XGB. Fig. 4 displays the PRCs of the aforementioned models, with the highest precision and recall being achieved by ExtraTrees, with only minor inconsistencies for classes 4% and 5% damage only, with AUC at 0.9989 and 0.9990 in Fig. 4(a). Considering our dataset was imbalanced, the PRC plots show the models' robustness in identifying the different classes in the experiments.

The ROC curve, another critical evaluation tool, plots the true positive rate against the false positive rate, highlighting the model's ability to distinguish between classes. The area under the ROC curve (AUC-ROC) serves as a measure of the model's overall performance, with values closer to 1 indicating near-perfect classification. Models achieving curves close to the top-left corner are considered highly effective. Fig. 3(d) refers to the performance of HGBM, and it shows near-perfect classification except for 4% and 5% faulty cases, which is almost equal to 0.9991, as does CatBoost in Fig. 3(e). When we compare the results of the top six models, ExtraTrees in Fig. 3(a) is the most robust, with its AUC of 4% and 5% both at 0.9998. Following that, RF in Fig. 3(b), MLP in Fig. 3(c), and XGB in Fig. 3(f) come after. These results demonstrate the models' capability to differentiate between normal and faulty cases with a high degree of accuracy.

In addition to these performance metrics, the explainability of the models was analyzed using SHAP, an explainable AI technique. SHAP

Table 1
Model comparison with full dataset.

S.No.	Model	Accuracy	Precision	F1	Accuracy_CV	Train Time (min)
1	ExtraTrees	0.9952	0.9952	0.9952	0.9949	4.19
2	Random Forest	0.9936	0.9937	0.9936	0.9934	53.62
3	MLP	0.9892	0.9892	0.9892	0.9906	36.37
4	HGBM	0.9890	0.9890	0.9890	0.9889	5.35
5	CatBoost	0.9888	0.9888	0.9888	0.9889	9.64
6	XGB	0.9873	0.9874	0.9873	0.9874	1.38
7	Decision Tree	0.9785	0.9785	0.9785	0.9756	10.49
8	Logistic Regression	0.9461	0.9462	0.9460	0.9463	1.67
9	QDA	0.8907	0.9204	0.8784	0.8566	0.59
10	SGD	0.8275	0.8190	0.8138	0.8274	1.25
11	LDA	0.8274	0.8324	0.8288	0.8286	0.60
12	Passive Aggressive	0.7958	0.7896	0.7909	0.8086	1.10
13	Perceptron	0.7847	0.7818	0.7810	0.8160	1.18
14	Ridge	0.6991	0.7231	0.6420	0.6994	0.05
15	Gaussian NB	0.4074	0.4816	0.3408	0.4043	0.05
16	AdaBoost	0.3535	0.3573	0.3182	0.3586	0.56

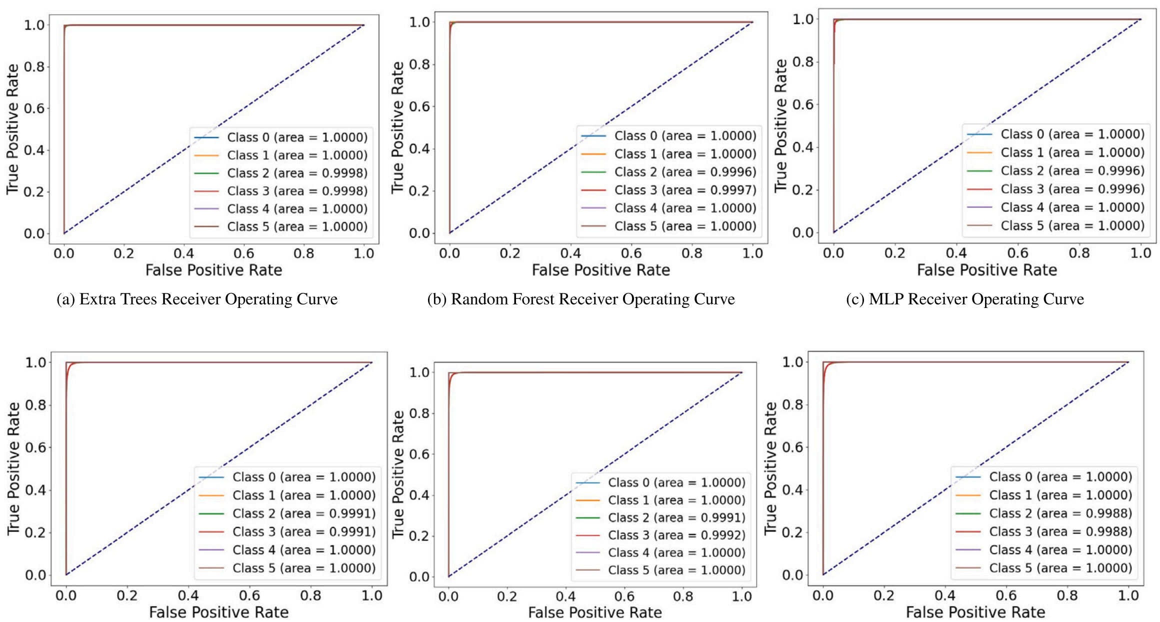

(a) Extra Trees Receiver Operating Curve (b) Random Forest Receiver Operating Curve (c) MLP Receiver Operating Curve

(d) HGBM Receiver Operating Curve (e) CatBoost Receiver Operating Curve (f) XGB Receiver Operating Curve

Fig. 3. Receiver operating curve results.

values were used to interpret the contribution of each feature to the model's predictions. XGB was selected as the reference model for this analysis. Fig. 5(a) illustrates the feature importance by displaying the mean absolute SHAP values across all samples, ranking features hierarchically from most to least impact. Fig. 5(b) further highlights the distribution and magnitude of SHAP values for the most influential features, showcasing their significance across individual instances. Lastly, Fig. 5(c) presents the average improvement in model accuracy attributed to each feature, demonstrating the gain or loss in information based on the feature's involvement in specific decision paths.

5. Discussion

The analysis of signal plots for normal, FC, and WC signals highlights key distinctions in their frequency and amplitude characteristics, offering insights into the features extracted for fault classification. Observations suggest that the coefficients exhibit a sinusoidal pattern, reflecting a strong correlation between the original signals and the extracted features. Across all plots, which span 10,000 points, notable differences in frequency and amplitude are evident. Faulty signals, for instance, exhibit higher frequencies while generally retaining their amplitude, distinguishing them from normal signals. In contrast, FC signals display substantial differences in both amplitude and frequency compared to their normal counterparts, indicating a pronounced distinction between these classes. For WC signals, the retention of negative values is a characteristic feature; however, while the amplitudes of normal and faulty WC signals appear similar, their corresponding time-domain signals differ significantly in amplitude. These variations underscore the value of the signal processing techniques employed, as they enhance the diversity and variance of the features fed into the ML models, thereby improving the robustness of fault classification.

Furthermore, it can be seen that the highest accuracies are obtained mostly by ensemble learning methods, and within that, the only difference lies within the approach of the learning method. The reason why Extra Trees has the highest accuracy due to its randomization property, where the splits are randomly done to ensure the highest variance, providing the maximum information. However, RF comes at a close second metric-wise based on its accuracy, precision, and F1 score. Since Extra Trees can be considered similar to RF in concept with a bit of a change in the split, it is unsurprisingly closer to the top range of accuracy. MLP comes at a third, and this is a completely different model compared to any of the other top models. Due to its neuron-like structure, MLP can be considered a learning network due to its continuous update of the weights during the learning process,

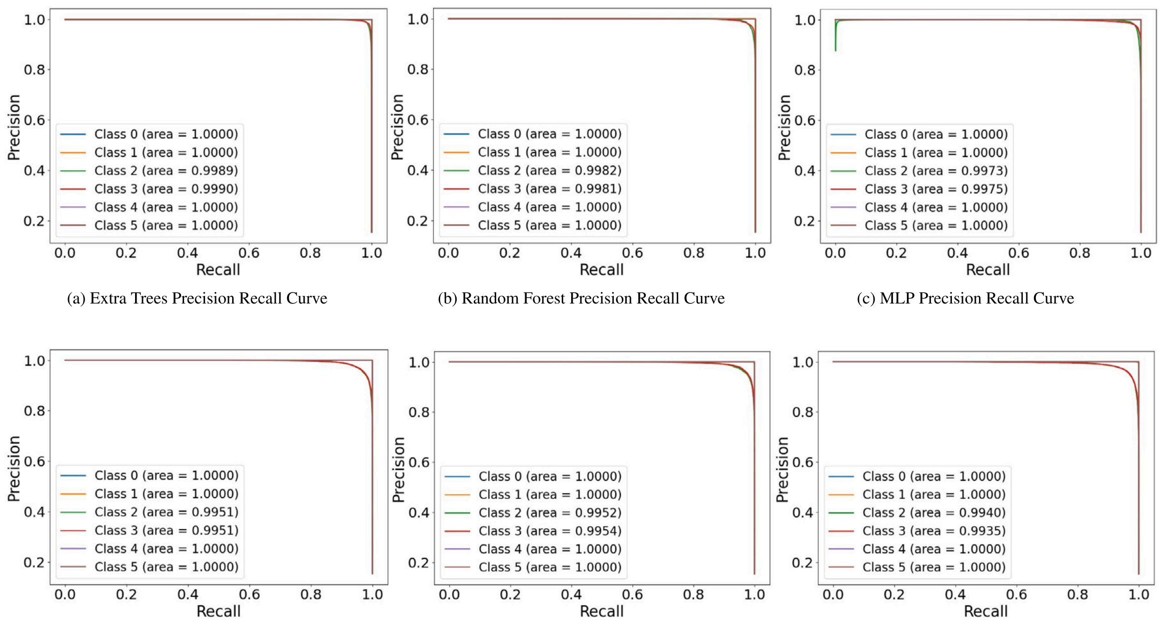

(d) HGBM Precision Recall Curve (e) CatBoost Precision Recall Curve (f) XGB Precision Recall Curve

Fig. 4. Precision recall curve results.

facilitating the reliance on every data while it is fed with the dataset. Additionally, in most of the cases where higher accuracy was obtained, we see the same consistency repeating throughout values of precision, F1 and cross validation, proving that these models indeed work appropriately for classification. The training time is another column listed in Table 1 where XGB claims the lowest training time among the set of models that achieved more than 90%. This makes XGB a viable option. However, ExtraTrees still holds the highest position with 4.19 min in training, proving its efficiency with a relatively low training time and accuracy of 99.52%, making it well balanced. However, RF and MLP still do have a high enough accuracy for application purposes, but it comes at a cost of higher training time. Since the purpose of this work is on diagnostic accuracy rather than deployment latency, it remains to be seen which models are quick and decisive in application. Since Extratrees is a threshold-based model where inference would mainly be comparisons between values, it would logically be faster than ensemble models like XGB and MLP, which require calculations at each step, affecting the speed depending on the type of processor used in deployment. On a final note, the Accuracy_CV confirms that there is no overfitting in any of the models as it performs cross validation, which means that it divides the dataset into sub-components, in this case five, and performs training and testing on each of those components and produces an accuracy value. Since the average accuracy value is approximately equal to the accuracy of the whole dataset, it confirms that the models were able to work perfectly with the training and testing dataset. Although Extra Trees outperformed the Random Forest model in terms of numerical performance, future work must include statistical significance tests to strengthen its usage. Moreover, there seems to be no bias towards the healthy class as the cross validation across k folds and the precision recall curves appear to be as highly robust as possible.

Table 2 shows the hyper-parameters that were used to train the ML models on. While grid search was implemented to test the model accuracy, it did not have significant different on the metrics as the major jump in accuracy was seen in the usage of spectral features on the current signal.

The SHAP plots provided in Figs. 5(a), 5(b), and 5(c) are used for discussion purposes to see how the dataset is explainable based on what features work best in the ML models used. The bar plot in Fig. 5(a) shows that Ic current signals' 2nd Fourier coefficient has the highest value and thus, it proves to be an important feature for the model for distinctive analysis. The *y*-axis in Fig. 5(a) is indicative of the most important features in descending order, till it reaches the point where the combination of all lowest features, specifically the bottom 141 features as shown in said figure, add up to 0.81 score after combination, meaning that they do not affect the ML's algorithm in classification of faults compared to Ic 2nd Fourier Coefficient, Ia standard deviation, Ib standard deviation, Ic standard deviation, Ic standard deviation, Ia 2nd Fourier Coefficient, Ib 10th Fourier Coefficient, Ib 2nd Fourier Coefficient, Ia 3rd Fourier Coefficient and Ib 9th Fourier Coefficient. Fig. 5(b) is a bit clearer on some randomly specified features to show their importance, namely current signal Ia, Ia standard deviation, Ib, Ia variance, Ic and Ia mean. It not only shows what contributes to the importance of a feature, but also what brings down the prediction values. Those with positive SHAP contribution are color coded in red, and otherwise blue. Fig. 5(c) is another plot importance diagram specifically catered to XGB. The top five features are listed in the plot, showing the importance of Ia signal energy in being distinctive. F score stands for the frequency with which the feature is used in the model's decision trees. The higher the F-score of a feature, the better XGB interprets it for classification, and this is represented by the aforementioned figure showing only the top ten most important features.

6. Conclusion

This paper presented a study distinguishing between multiple severity of stator winding faults in induction motors using machine learning techniques. A unique and comprehensive experimental dataset was processed through signal processing-based feature engineering, where Fourier coefficients, wavelet coefficients, and statistical features were collected to maximize fault related information. Multiple machine learning models, including Random Forest, XGB and Multilayer Perceptron were evaluated and compared, with Extra Trees achieving the highest performance. It achieved 99.52% accuracy with a training time of 4.19 min, The top models were further validated using precision, F1-score, cross-validation, ROC, and PR curves to ensure robustness. Additionally, SHAP-based explainable AI analysis was conducted to

Table 2
Optimized hyperparameters used for training purposes of healthy and faulty data.

Model	Hyperparameter(s)	Value(s)
Ridge	alpha	1
Quadratic Discriminant Analysis	priors	None
XGBoost	n_estimators	None
CatBoost	verbose	FALSE
Gaussian Naive Bayes	priors, var_smoothing	None, 1×10^{-9}
Logistic Regression	max_iter, solver	100, lbfgs
Histogram Gradient Boosting	learning_rate, max_features, loss	0.1, 1, hinge
Linear Discriminant Analysis	n_components, solver, priors	None, svd, None
Bagging	max_samples, max_features, n_estimators	1, 1, 10
AdaBoost	algorithm, learning_rate, n_estimators	SAMME.R, 1, 50
Perceptron	alpha, l1_ratio, max_iter	0.0001, 0.15, 1000
Passive Aggressive	C, max_iter, validation_fraction, loss	1, 1000, 0.1, hinge
K-nearest Neighbors	n_neighbors, leaf_size, p, weights, metric	5, 30, 2, uniform, minkowski
Stochastic Gradient Descent	alpha, epsilon, l1_ratio, learning_rate, loss, max_iter	0.0001, 1, 0.15, optimal, hinge, 1000
Decision Tree	class_weight, criterion, max_depth, max_features, max_leaf_nodes, min_impurity_decrease	None, gini, None, None, None, 0
Random Forest, Extra Trees	bootstrap, criterion, max_features, min_samples_leaf, min_samples_split, n_estimators	TRUE, gini, sqrt, 1, 2, 100
Multilayer Perceptron	activation, alpha, beta_1, beta_2, epsilon, hidden_layer_sizes, learning_rate, learning_rate_init, max_iter, momentum	relu, 0.0001, 0.9, 0.999, 1×10^{-8}, (100,), constant, 0.001, 200, 0.9

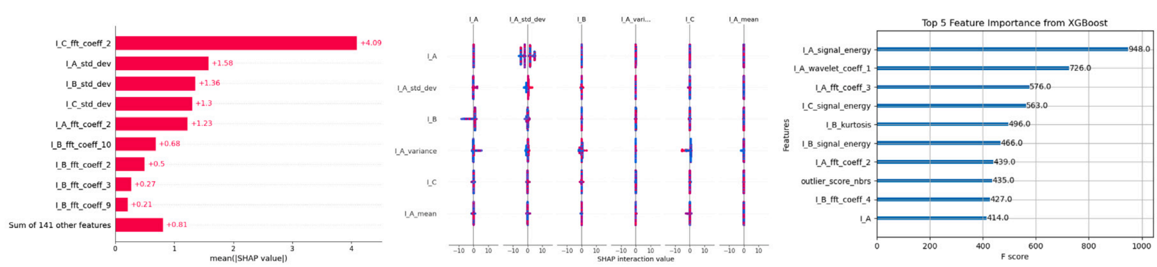

(a) SHAP Bar Plot (b) SHAP Summary Plot (c) SHAP Plot Importance

Fig. 5. Combined SHAP explanations.

identify the most influential features contributing to accurate classification, enhancing the interpretability and transparency of the proposed framework.

Future research may concentrate on expanding this framework to real-time deployment in industrial environments via embedded or edge-AI implementations that facilitate online monitoring. In order to do away with manual feature extraction and enable end-to-end learning, future studies may explore the application of deep learning architectures, such as 1D-CNNs or hybrid CNN-transformer models. Generalization would be strengthened by expanding the dataset to cover a variety of operational situations, motor ratings, and load conditions. To further improve practical applicability, future work may investigate incorporating transfer learning for cross-motor adaptability and predictive maintenance modules for early forecasting of impending failures.

CRediT authorship contribution statement

Rehaan Hussain: Writing – original draft, Methodology, Investigation, Formal analysis, Conceptualization. **Mohammed Yaqoob:** Methodology. **Mohammed Ishaq:** Formal analysis. **Mohammad Al-shaikh Saleh:** Investigation. **Shady S. Refaat:** Writing – review & editing, Supervision, Methodology.

Declaration of competing interest

The authors declare the following financial interests/personal relationships which may be considered as potential competing interests: Shady S. Refaat reports article publishing charges was provided by University of Hertfordshire. Shady S. Refaat reports a relationship with University of Hertfordshire School of Physics Engineering and Computer Science that includes: employment. N/A If there are other authors, they declare that they have no known competing financial interests or personal relationships that could have appeared to influence the work reported in this paper.

Acknowledgment

This work was supported by National Priorities Research Program grant [13S-0116-200085] from the Qatar National Research Fund (a member of Qatar Foundation). The statements made herein are solely the responsibility of the authors.

Data availability

Data will be made available on request.

References

[1] Kamalapur G, Muni TV, Kumar PR, Parimala V, Kishore KV, Aspalli M. A novel neuro fuzzy method DTC of induction motor drive for efficient torque response. In: 2022 3rd international conference for emerging technology. IEEE; 2022, p. 1–7.
[2] Singh V, Gangsar P, Porwal R, Atulkar A. Artificial intelligence application in fault diagnostics of rotating industrial machines: A state-of-the-art review. J Intell Manuf 2023;34(3):931–60.
[3] Hussain R, Saleh MA, Refaat SS. Induction motor multi incipient fault detection based on gradient boosting algorithms. In: IECON 2024-50th annual conference of the IEEE industrial electronics society. IEEE; 2024, p. 1–6.
[4] Yu Z, Lei N, Mo Y, Xu X, Li X, Huang B. Feature extraction based on self-supervised learning for remaining useful life prediction. J Comput Inf Sci Eng 2024;24(2).
[5] Shifat TA, Hur J-W. ANN assisted multi sensor information fusion for BLDC motor fault diagnosis. IEEE Access 2021;9:9429–41.
[6] Sharma NR, Bhalja BR, Malik OP. Machine learning-based severity assessment and incipient turn-to-turn fault detection in induction motors. IEEE Trans Energy Convers 2024.
[7] Rafiei V, Khoshlessan M, Caicedo-Narvaez C, Fahimi B. Detection of inter-turn short circuit in stator windings of electric machines using magnetic symmetry index and machine learning methods. IEEE Trans Energy Convers 2024.
[8] Chen L, Shen J, Xu G, Chi C, Feng Q, Zhou Y, Deng Y, Wen H. Induction motor stator winding inter-tern short circuit fault detection based on start-up current envelope energy. Sensors 2023;23(20):8581.
[9] Aswad RA, Jassim BM. Detection and localization of the stator winding inter-turn fault in induction motors based on parameters estimation using genetic algorithm. J Inst Eng (India): Ser B 2022;103(2):405–14.
[10] Hussein AM, Obed AA, Zubo RH, Al-Yasir YI, Saleh AL, Fadhel H, Sheikh-Akbari A, Mokryani G, Abd-Alhameed RA. Detection and diagnosis of stator and rotor electrical faults for three-phase induction motor via wavelet energy approach. Electronics 2022;11(8):1253.
[11] Cherif H, Benakcha A, Laib I, Chehaidia SE, Menacer A, Soudan B, Olabi A. Early detection and localization of stator inter-turn faults based on discrete wavelet energy ratio and neural networks in induction motor. Energy 2020;212:118684.
[12] Almounajjed A, Sahoo AK, Kumar MK. Diagnosis of stator fault severity in induction motor based on discrete wavelet analysis. Measurement 2021;182:109780.
[13] Das AK, Das S, Pradhan AK, Chatterjee B, Dalai S. RPCNNet: A deep learning approach to sense minor stator winding interturn fault severity in induction motor under variable load condition. IEEE Sensors J 2023;23(4):3965–72.
[14] Radhi AT, Zayer WH. Faults diagnosis in stator windings of high speed solid rotor induction motors using fuzzy neural network. Int J Power Electron Drive Syst 2021;12(1):597.
[15] Hussain M, Soother DK, Kalwar IH, Memon TD, Memon ZA, Nisar K, Chowdhry BS. Stator winding fault detection and classification in three-phase induction motor. Intell Autom Soft Comput 2021;29(3):869–83.
[16] Singh M, Shaik AG. Incipient fault detection in stator windings of an induction motor using stockwell transform and SVM. IEEE Trans Instrum Meas 2020;69(12):9496–504.
[17] Lee S-h, Wang Y-q, Song J-i. Fourier and wavelet transformations application to fault detection of induction motor with stator current. J Central South Univ Technol 2010;17(1):93–101.
[18] Zhang Z, Wang Y, Wang K. Fault diagnosis and prognosis using wavelet packet decomposition, Fourier transform and artificial neural network. J Intell Manuf 2013;24(6):1213–27.
[19] Megahed A, Moussa AM, Elrefaie H, Marghany Y. Selection of a suitable mother wavelet for analyzing power system fault transients. In: 2008 IEEE power and energy society general meeting-conversion and delivery of electrical energy in the 21st century. IEEE; 2008, p. 1–7.
[20] Debnath L. Wavelets and signal processing. Springer Science & Business Media; 2003.
[21] Fernandes AAT, Figueiredo Filho DB, Rocha ECd, Nascimento WdS. Read this paper if you want to learn logistic regression. Rev Sociol E Política 2021;28:006.
[22] Zhang W, Yin Z, Sheng Z, Li Y, Ouyang W, Li X, Tao Y, Yang Z, Cui B. Graph attention multi-layer perceptron. In: Proceedings of the 28th ACM SIGKDD conference on knowledge discovery and data mining. 2022, p. 4560–70.
[23] Zhao S, Zhang B, Yang J, Zhou J, Xu Y. Linear discriminant analysis. Nat Rev Methods Prim 2024;4(1):70.
[24] Ghosh A, SahaRay R, Chakrabarty S, Bhadra S. Robust generalised quadratic discriminant analysis. Pattern Recognit 2021;117:107981.
[25] Cunningham P, Delany SJ. K-nearest neighbour classifiers-a tutorial. ACM Comput Surv 2021;54(6):1–25.
[26] Costa VG, Pedreira CE. Recent advances in decision trees: An updated survey. Artif Intell Rev 2023;56(5):4765–800.
[27] Hu J, Szymczak S. A review on longitudinal data analysis with random forest. Brief Bioinform 2023;24(2):bbad002.
[28] Zhang J, Ma X, Zhang J, Sun D, Zhou X, Mi C, Wen H. Insights into geospatial heterogeneity of landslide susceptibility based on the SHAP-XGBoost model. J Environ Manag 2023;332:117357.
[29] Guo Z, Wang X, Ge L. Classification prediction model of indoor PM2. 5 concentration using CatBoost algorithm. Front Built Environ 2023;9:1207193.
[30] Reddy EMK, Gurrala A, Hasitha VB, Kumar KVR. Introduction to naive Bayes and a review on its subtypes with applications. Bayesian Reason Gaussian Process Mach Learn Appl 2022;1–14.
[31] Tian Y, Zhang Y, Zhang H. Recent advances in stochastic gradient descent in deep learning. Mathematics 2023;11(3):682.
[32] Saeed U, Jan SU, Lee Y-D, Koo I. Fault diagnosis based on extremely randomized trees in wireless sensor networks. Reliab Eng Syst Saf 2021;205:107284.
[33] Gupta S, Meel P. Fake news detection using passive-aggressive classifier. In: Inventive communication and computational technologies: proceedings of ICICCT 2020. Springer; 2021, p. 155–64.
[34] Rosenblatt F, Papert S. In: Perceptron, vol. 9, April; 2021.
[35] Arashi M, Roozbeh M, Hamzah NA, Gasparini M. Ridge regression and its applications in genetic studies. PLoS One 2021;16(4):e0245376.
[36] Ngo G, Beard R, Chandra R. Evolutionary bagging for ensemble learning. Neurocomputing 2022;510:1–14.
[37] Ding Y, Zhu H, Chen R, Li R. An efficient AdaBoost algorithm with the multiple thresholds classification. Appl Sci 2022;12(12):5872.
[38] Nhat-Duc H, Van-Duc T. Comparison of histogram-based gradient boosting classification machine, random forest, and deep convolutional neural network for pavement raveling severity classification. Autom Constr 2023;148:104767.
[39] Azad M, Chikalov I, Hussain S, Moshkov M. Entropy-based greedy algorithm for decision trees using hypotheses. Entropy 2021;23(7):808.
[40] Genuer R, Poggi J-M, Genuer R, Poggi J-M. Random forests. Springer; 2020.
[41] Guryanov A. Histogram-based algorithm for building gradient boosting ensembles of piecewise linear decision trees. In: Analysis of images, social networks and texts: 8th international conference, AIST 2019, kazan, Russia, July 17–19, 2019, revised selected papers 8. Springer; 2019, p. 39–50.
[42] Desai M, Shah M. An anatomization on breast cancer detection and diagnosis employing multi-layer perceptron neural network (MLP) and convolutional neural network (CNN). Clin EHealth 2021;4:1–11.
[43] Lu C, Fei J, Meng X, Li Y, Liu Z. Thermal error prediction and compensation of digital twin laser cutting based on T-XGBoost. Sensors 2022;22(18):7022.